Supporting information

Nano-design of quantum dot-based photocatalysts for hydrogen generation using advanced surface molecular chemistry

Weili Yu, Dalal Noureldine, Tayirjan Isimjan,* Bin Lin, Silvano Del Gobbo, Mutalifu Abulikemu, Mohamed Nejib Hedhili, Dalaver Hussain Anjum, and Kazuhiro Takanabe*

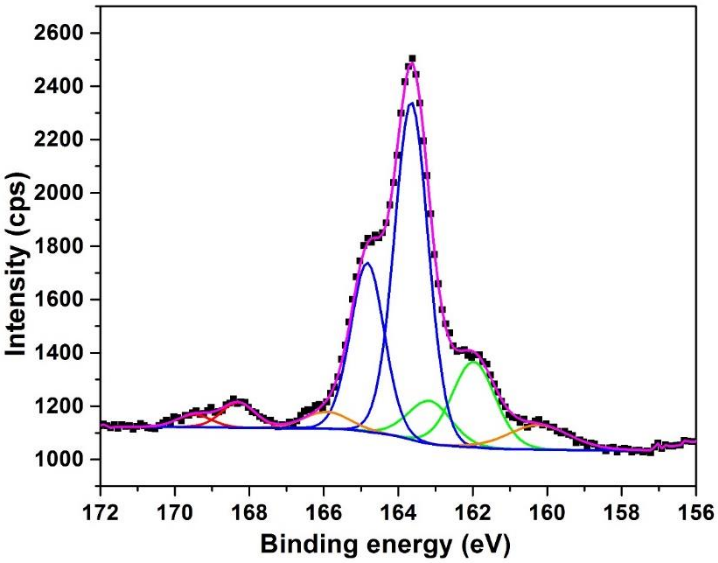

Figure S1. High resolution XP spectra of the S 2p core level of CdSe-TiO_2-MPTMS powder (without ZnS shell of QD).

As shown in **Figure S1**, we attempted to provide evidence of the functionalization of the CdSe quantum dots (without ZnS shell). The S 2p photoemission signal overlaps with the Se 3p signal from CdSe. The spectrum consists of three (S $2p_{3/2}$–S $2p_{1/2}$) spin-orbit doublets and one (Se $3p_{3/2}$–Se $3p_{1/2}$) spin-orbit doublet. The doublet separation at 5.8 eV and a fixed area ratio equal to 2:1 were used for the (Se $3p_{3/2}$–Se $3p_{1/2}$) doublet. The S $2p_{3/2}$ components were located at binding energy values of 162.0, 163.6 and 168.3 eV, respectively. The peaks at 163.6 and 168.3 eV correspond to unbound thiols and sulfates, respectively, whereas the new peak located at 162.0 eV is assigned to Cd-S bonds.[1-3] CdSe quantum dots capped with mercaptopropyl porous phosphate heterostructure (PPH-SH) show similar structures at the same binding energy that corresponds to the formation of PPH-S-CdSe nanocomposites.[2] Furthermore, the binding energies of the Se $3p_{3/2}$ component at 160.2 eV and the Cd $3d_{5/2}$ component at 405.2 eV (results not shown) are in good agreement with previously reported values for CdSe.[4-6]

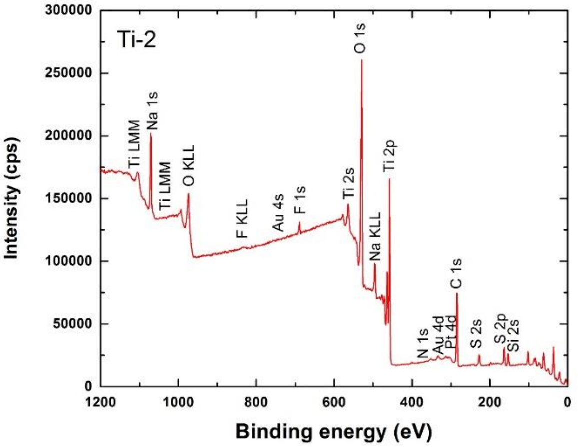
Ti-2
Intensity (cps)
Binding energy (eV)
300000
250000
200000
150000
100000
50000
0
1200
1000
800
600
400
200
0
Ti LMM
Na 1s
Ti LMM
O KLL
F KLL
Au 4s
F 1s
Ti 2s
O 1s
Ti 2p
Na KLL
C 1s
N 1s
Au 4d
Pt 4d
S 2s
S 2p
Si 2s

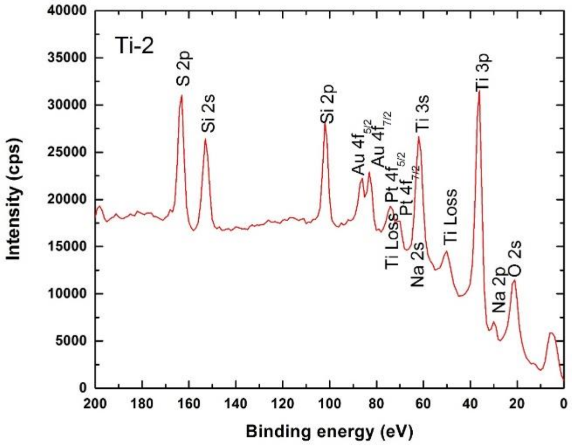
Ti-2
Intensity (cps)
Binding energy (eV)
40000
35000
30000
25000
20000
15000
10000
5000
0
200
180
160
140
120
100
80
60
40
20
0
S 2p
Si 2s
Si 2p
Au $4f_{5/2}$
Au $4f_{7/2}$
Pt $4f_{5/2}$
Pt $4f_{7/2}$
Ti Loss
Ti 3s
Na 2s
Ti Loss
Ti 3p
Na 2p
O 2s

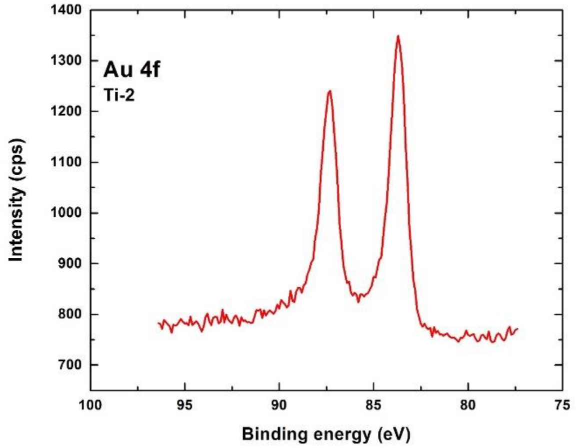
Au 4f
Ti-2
Intensity (cps)
Binding energy (eV)
1400
1300
1200
1100
1000
900
800
700
100
95
90
85
80
75

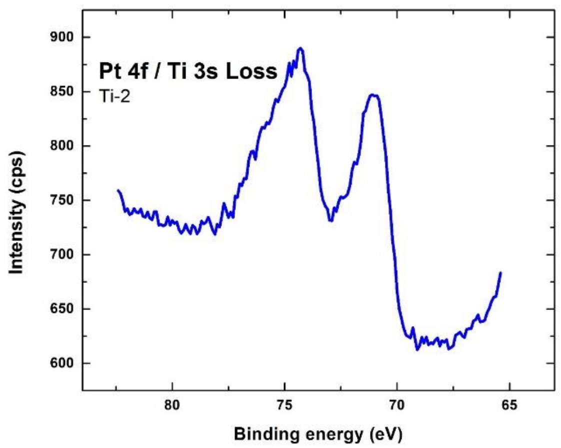
Pt 4f / Ti 3s Loss
Ti-2
Intensity (cps)
Binding energy (eV)
900
850
800
750
700
650
600
80
75
70
65

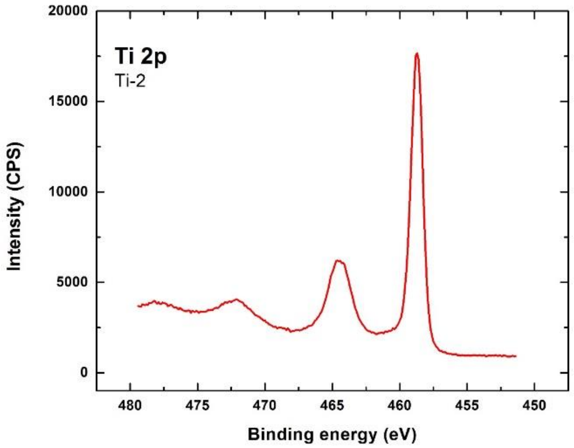
Ti 2p
Ti-2
Intensity (CPS)
Binding energy (eV)
20000
15000
10000
5000
0
480
475
470
465
460
455
450

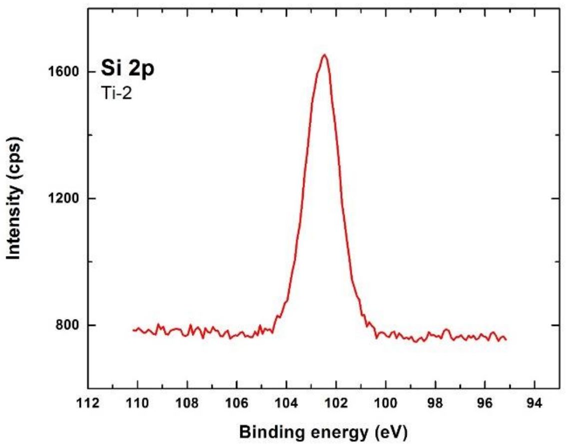
Si 2p
Ti-2
Intensity (cps)
Binding energy (eV)
1600
1200
800
112
110
108
106
104
102
100
98
96
94

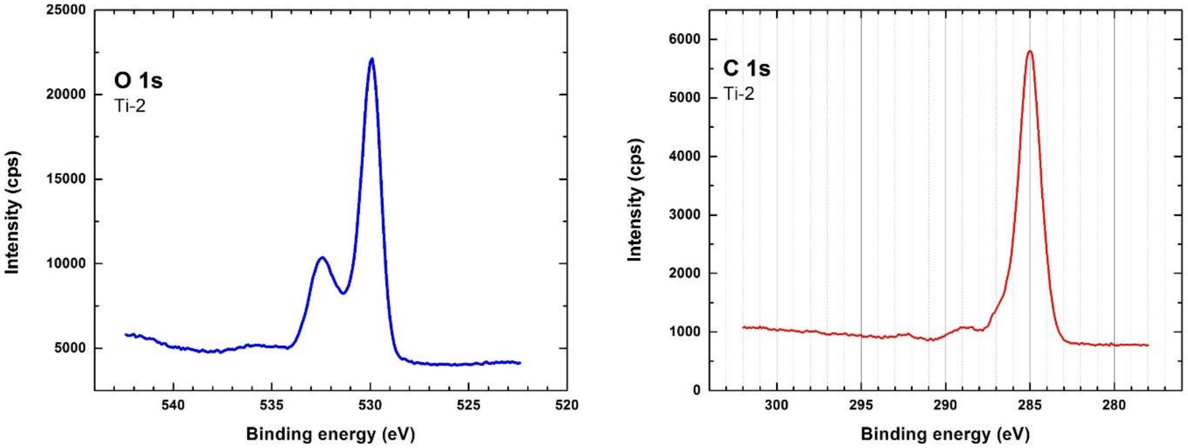

Figure S2. High resolution XP spectra of the wide scan and detailed spectra for each component of Ti-2.

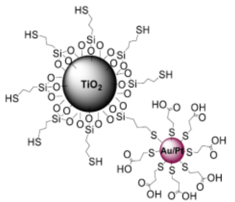

Ti-2

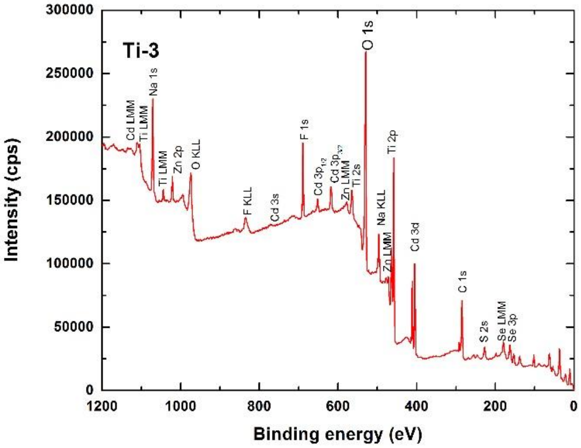
Ti-3
Cd LMM
Ti LMM
Na 1s
Ti LMM
Zn 2p
O KLL
F KLL
Cd 3s
F 1s
Cd 3p1/2
Cd 3p3/2
Zn LMM
Ti 2s
O 1s
Na KLL
Zn LMM
Ti 2p
Cd 3d
C 1s
S 2s
Se LMM
Se 3p
Intensity (cps)
300000
250000
200000
150000
100000
50000
0
1200
1000
800
600
400
200
0
Binding energy (eV)

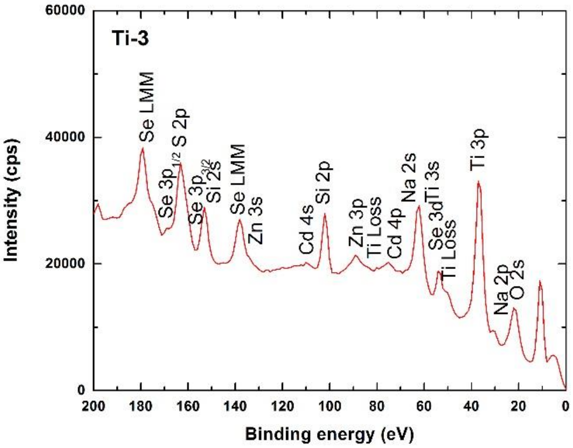
Ti-3
Se LMM
Se 3p1/2
S 2p
Se 3p3/2
Si 2s
Se LMM
Zn 3s
Cd 4s
Si 2p
Zn 3p
Ti Loss
Cd 4p
Na 2s
Se 3d
Ti 3s
Ti Loss
Ti 3p
Na 2p
O 2s
Intensity (cps)
60000
40000
20000
0
200
180
160
140
120
100
80
60
40
20
0
Binding energy (eV)

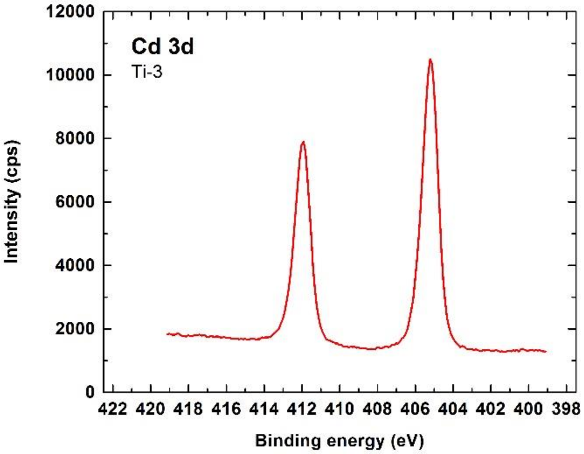
Cd 3d
Ti-3
Intensity (cps)
12000
10000
8000
6000
4000
2000
0
422
420
418
416
414
412
410
408
406
404
402
400
398
Binding energy (eV)

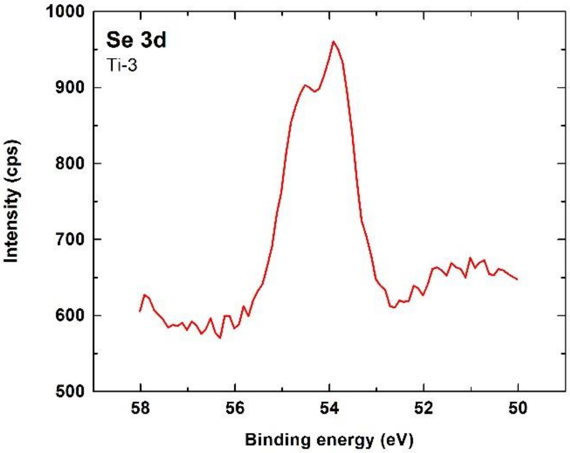
Se 3d
Ti-3
Intensity (cps)
1000
900
800
700
600
500
58
56
54
52
50
Binding energy (eV)

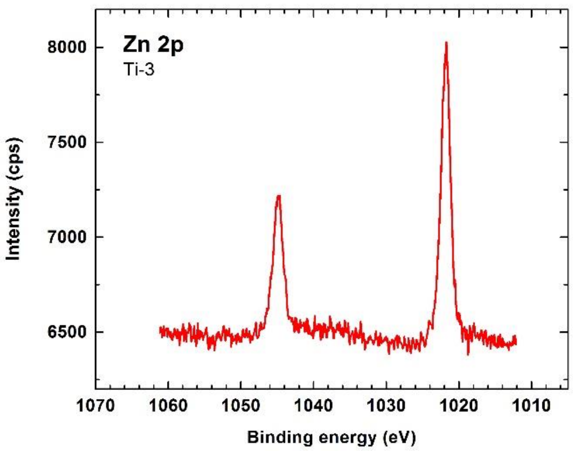
Zn 2p
Ti-3
Intensity (cps)
8000
7500
7000
6500
1070
1060
1050
1040
1030
1020
1010
Binding energy (eV)

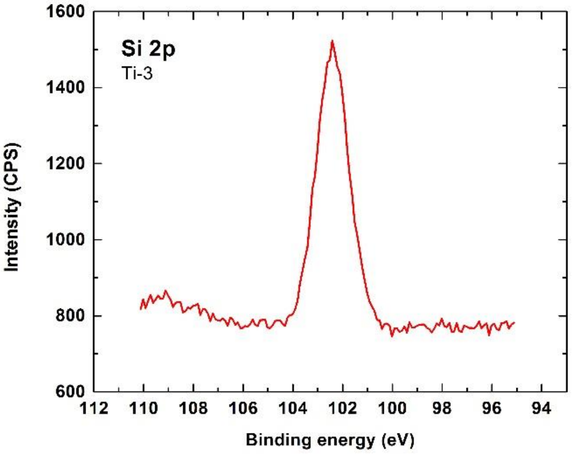
Si 2p
Ti-3
Intensity (CPS)
1600
1400
1200
1000
800
600
112
110
108
106
104
102
100
98
96
94
Binding energy (eV)

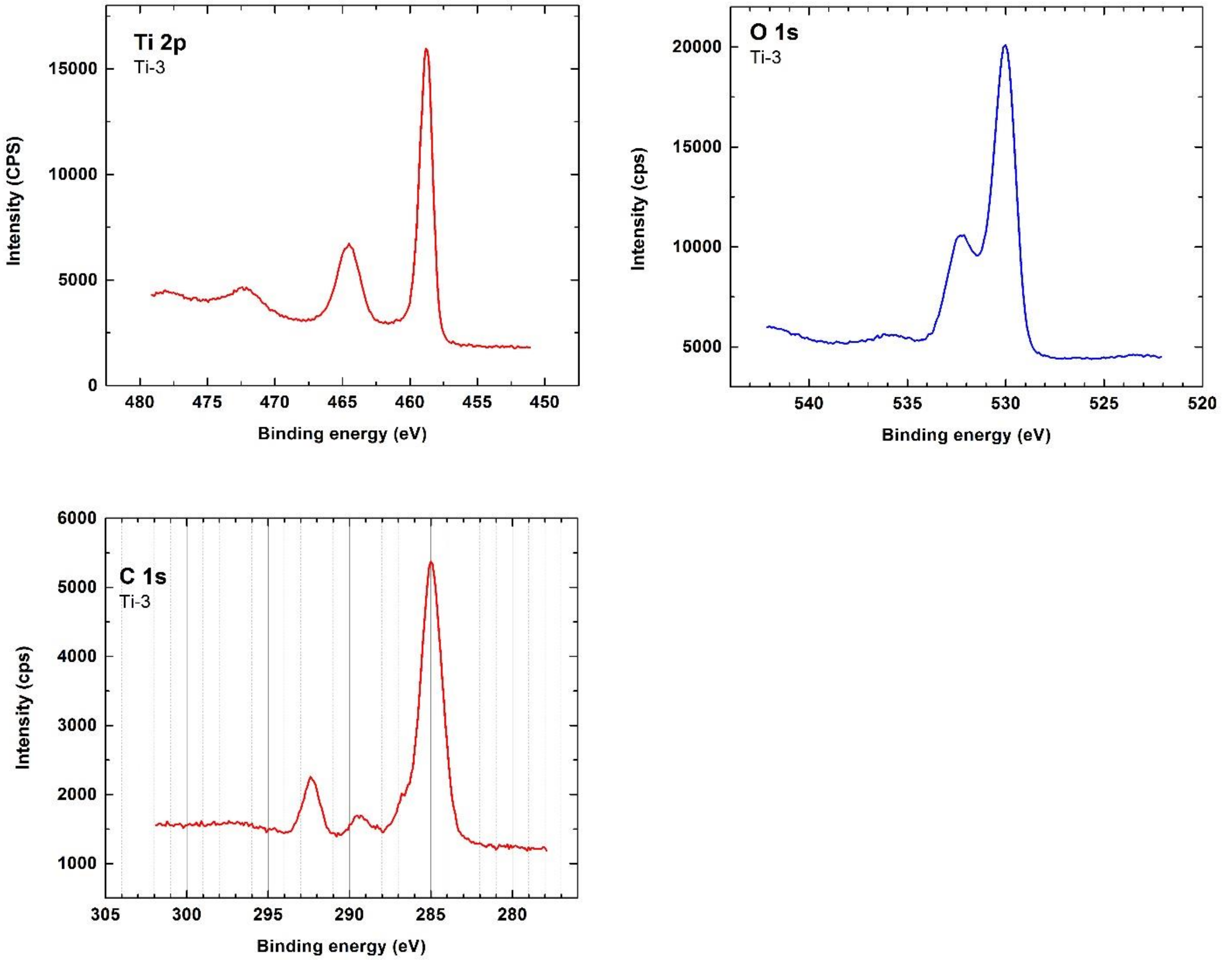

Figure S3. High resolution XP spectra of the wide scan and detailed spectra for each component of Ti-3.

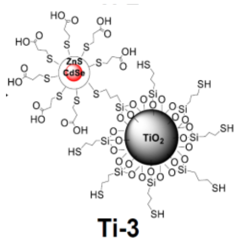

Ti-3

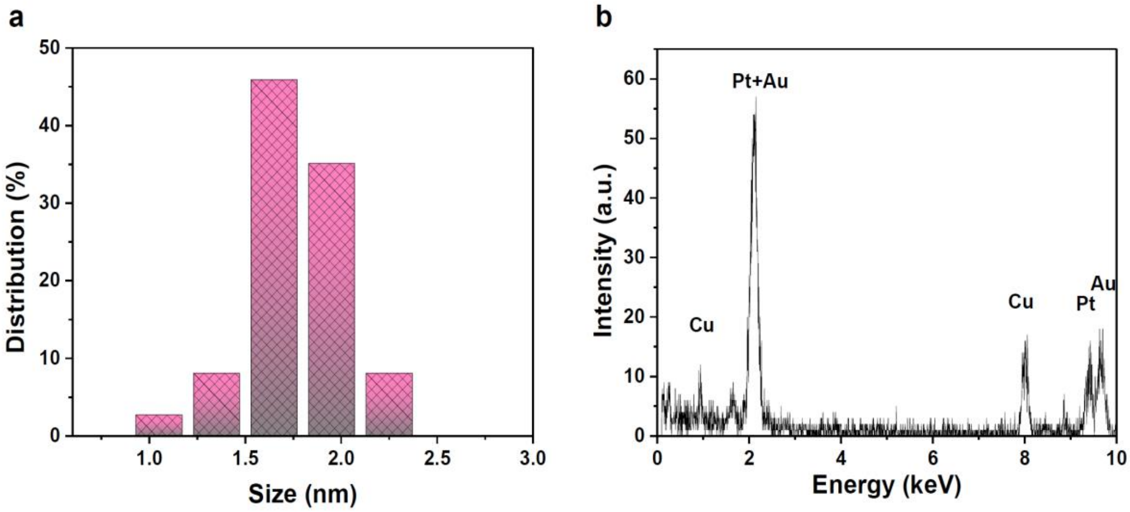

Figure S4. a) Size distribution and b) EDS spectrum of the Au/Pt alloy NCs.

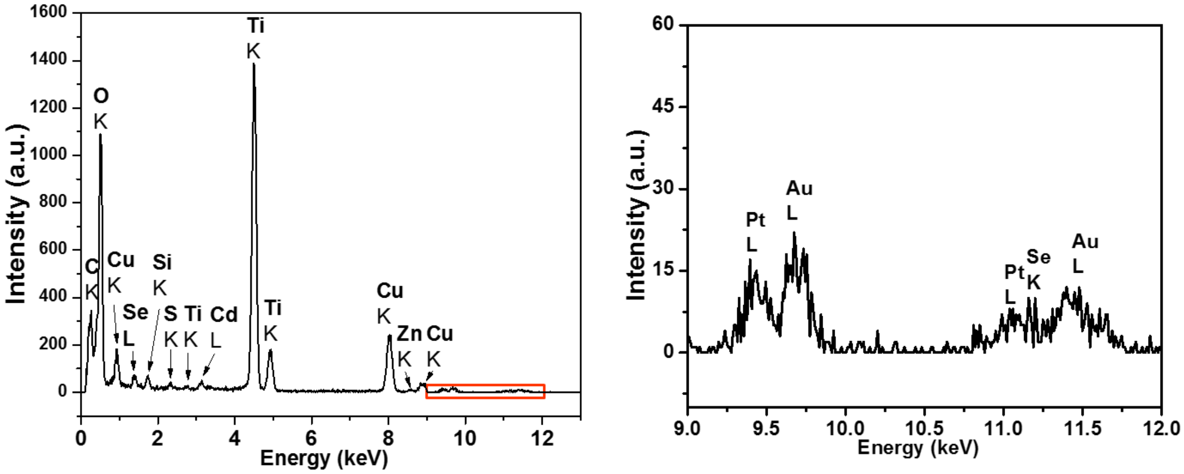

Figure S5. EDS spectrum of the **Ti-4** sample.

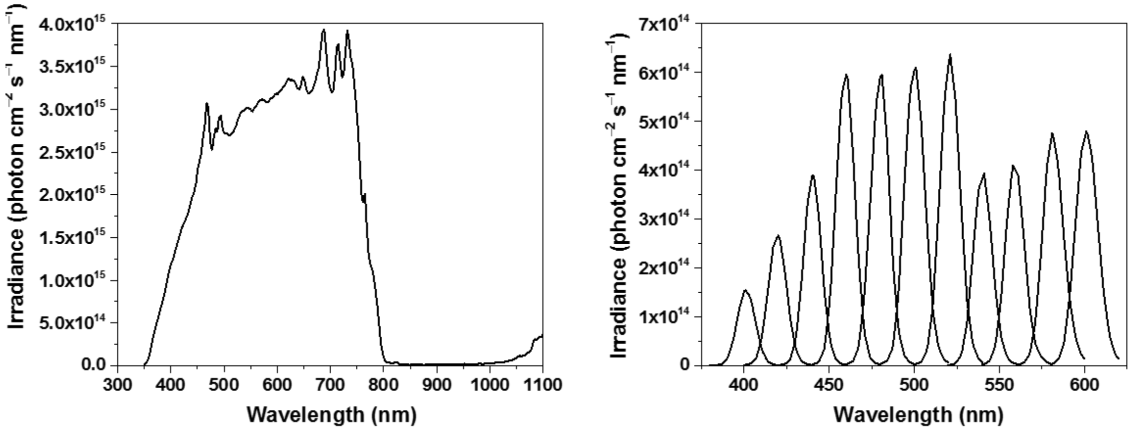

Figure S6. Photon irradiance of the light source (ASAHI) over the full wavelength range used and with band pass filters for QE measurements.

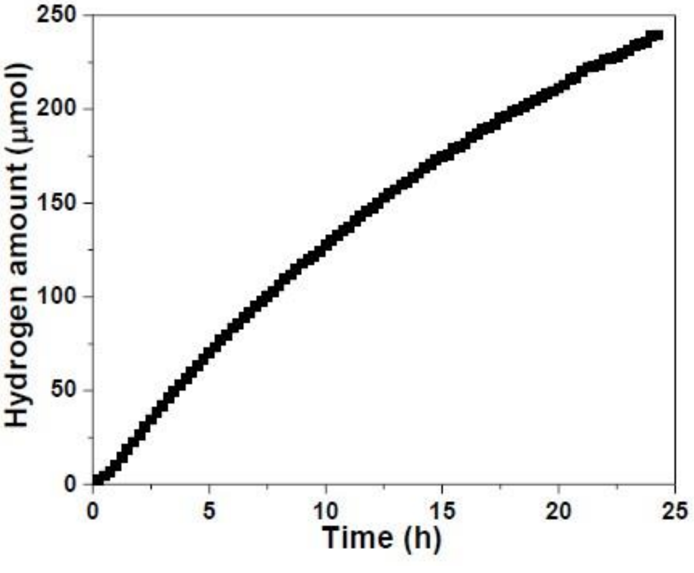

Figure S7. Hydrogen evolution of Au/Pt-TiO_2-CdSe complexes.

Average evolution rate of hydrogen: 9.8 μmol h^{-1}.

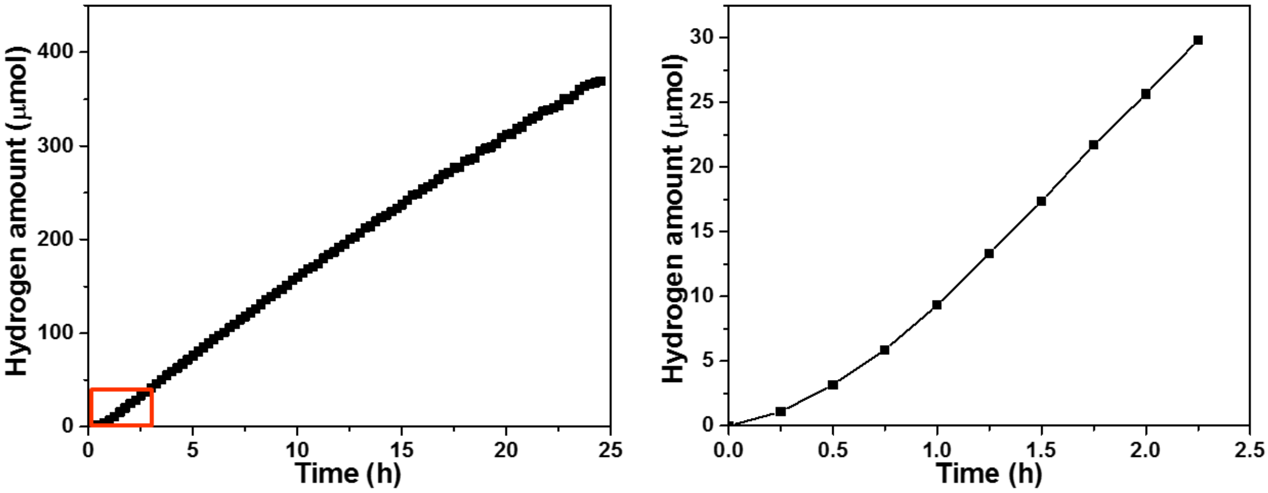

Figure S8. Hydrogen evolution of Au/Pt-CdSe@ZnS complexes.

Average evolution rate of hydrogen: 15.6 μmol h^{-1}.

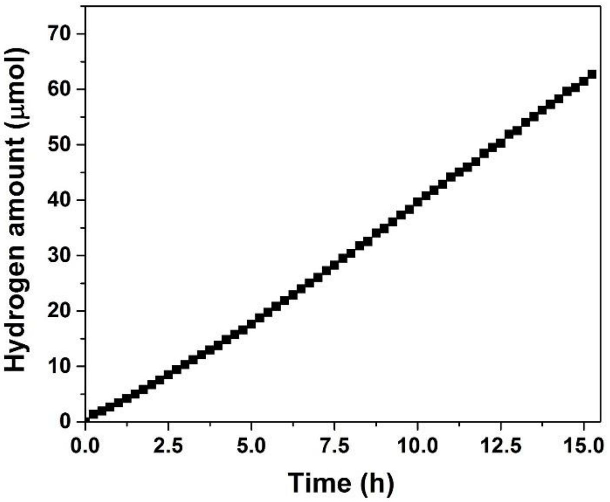

Figure S9. Hydrogen evolution of CdSe@ZnS-TiO_2-Au/Pt complexes (**Ti-4**) in an aqueous MeOH solution (10% v/v).

Average evolution rate of hydrogen: 4.2 μmol h^{-1}. Amounts: 30 mg **Ti-4** (590 nm) in 25 ml of an aqueous solution containing Na_2S (0.5 M) and Na_2SO_3 (0.5 M).

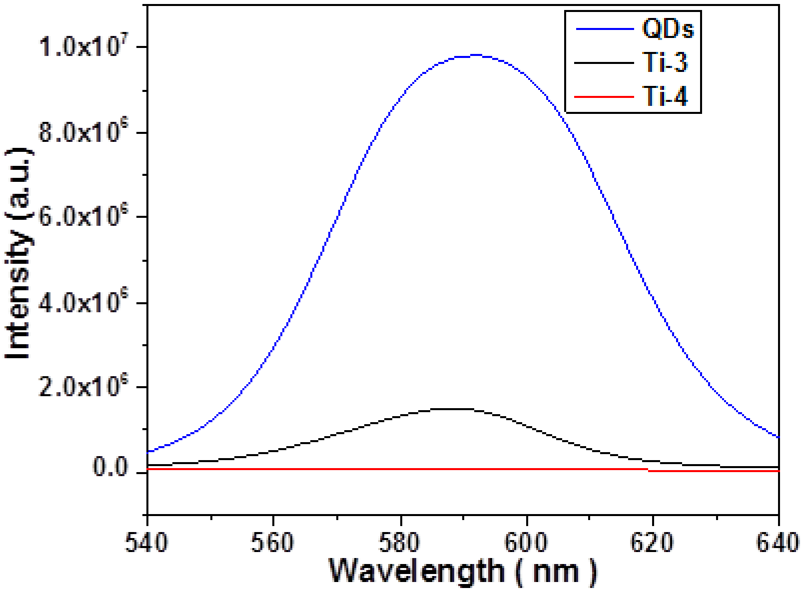

Figure S10. Photoluminescence of QDs, sample **Ti-3** and sample **Ti-4**.

Table S1. Average sizes of different ZnS@CdSe QDs obtained from the chemical provider Sigma-Aldrich.

PL peak	560 nm	590 nm	610 nm	640 nm
Size (nm)	3.4	4.0	5.2	6.3

Note: The monolayer thickness of the ZnS shell was calculated according to the distance of 3.1 Å between consecutive planes along the [002] axis in bulk wurtzite ZnS. According to the manufacturer, a ZnS shell measuring 2 to 3 monolayers in thickness was epitaxially grown in solution on the CdSe core. Therefore, the average shell thickness was approximately 1.2–1.9 nm.[10]

Table S2. ICP data (wt%) for **Ti-4** with ZnS@CdSe QDs of different sizes.

Sample labels	Au	Pt	Se	Cd	S	Ti	Zn	ZnS@CdSe[a]	Au+Pt[b]
Ti-4 (QD560)	0.38	0.37	0.70	1.7	2.8	45.7	0.29	2.8	0.75
Ti-4 (QD590)	0.39	0.37	0.80	2.1	3.0	47.8	0.30	3.4	0.76
Ti-4 (QD610)	0.37	0.40	0.76	2.1	3.1	47.0	0.31	3.3	0.77
Ti-4 (QD640)	0.37	0.37	0.83	1.9	3.2	45.1	0.32	3.2	0.74

[a] The weight percent of ZnS was calculated based on Zn metal; [b] the sum of the Au and Pt weight percents.

Reference (Supporting information)

1. Stoev, M. and A. Katerski, *XPS and XRD study of photoconductive CdS films obtained by a chemical bath deposition process.* Journal of Materials Chemistry, 1996. **6**(3): p. 377-380.

2. Algarra, M., et al., *Solid luminescent CdSe-thiolated porous phosphate heterostructures. Application in fingermark detection in different surfaces.* Surface and Interface Analysis, 2013. **45**(2): p. 612-618.

3. Espinós, J.P., et al., *X-ray photoelectron spectroscopy study of the nucleation processes and chemistry of CdS thin films deposited by sublimation on different solar cell substrate materials.* Journal of Vacuum Science & Technology A, 2006. **24**(4): p. 919-928.

4. Rupp, H. and U. Weser, *X-ray photoelectron spectroscopy of some selenium containing amino acids.* Bioinorganic Chemistry, 1975. **5**(1): p. 21-32.

5. Katari, J.E.B., V.L. Colvin, and A.P. Alivisatos, *X-ray Photoelectron Spectroscopy of CdSe Nanocrystals with Applications to Studies of the Nanocrystal Surface.* The Journal of Physical Chemistry, 1994. **98**(15): p. 4109-4117.

6. Zhu, C.-Q., et al., *Facile Phosphine-Free Synthesis of CdSe/ZnS Core/Shell Nanocrystals Without Precursor Injection.* Nanoscale Research Letters, 2008. **3**(6): p. 213 - 220.

7. Cingarapu, S., et al., *Synthesis of CdSe/ZnS and CdTe/ZnS Quantum Dots: Refined Digestive Ripening.* Journal of Nanomaterials, 2012. **2012**: p. 12.

8. Sambur, J.B. and B.A. Parkinson, *CdSe/ZnS Core/Shell Quantum Dot Sensitization of Low Index TiO2 Single Crystal Surfaces.* Journal of the American Chemical Society, 2010. **132**(7): p. 2130-2131.